Electronic Supplementary Material (ESI) for Journal of Materials Chemistry C.

Supporting Information

The dibenzo heterocyclic-terminated spiro-typed hole transporting materials for perovskite solar cells

Yongpeng Liang[1], Jianlin Chen[1], Xianfu Zhang, Mingyuan Han, Rahim Ghadari, Nan Wu, Ying Wang, Ying Zhou, Xuepeng Liu*, Songyuan Dai

[a] *School of New Energy, North China Electric Power University, Beijing 102206, China. E-mail: liuxuepeng@ncepu.edu.cn*
[b] *Computational Chemistry Laboratory, Department of Organic and Biochemistry, Faculty of Chemistry, University of Tabriz, Tabriz, 5166616471, Iran.*

Yongpeng Liang and Jianlin Chen contributed equally to this study.

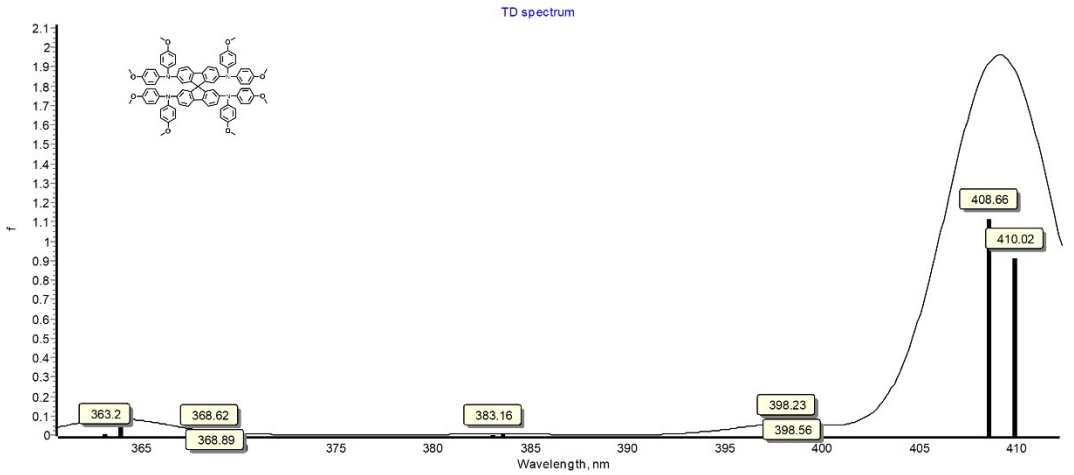

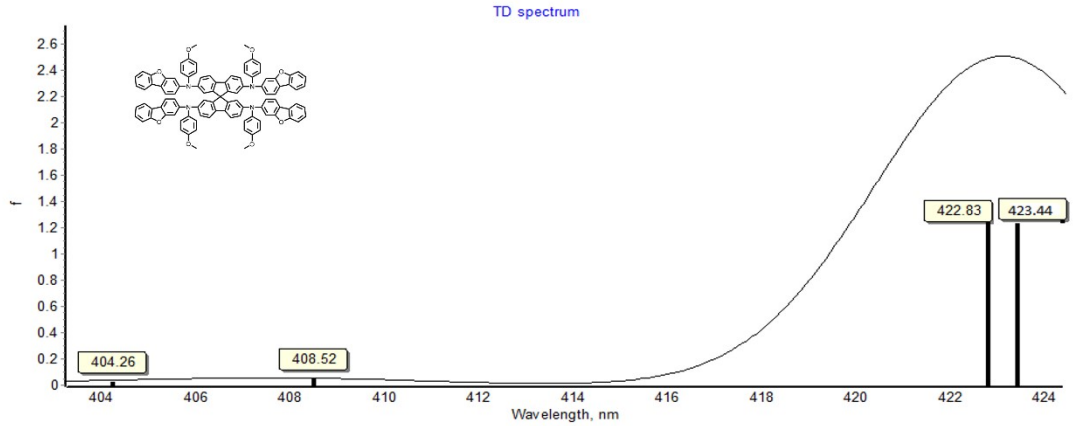

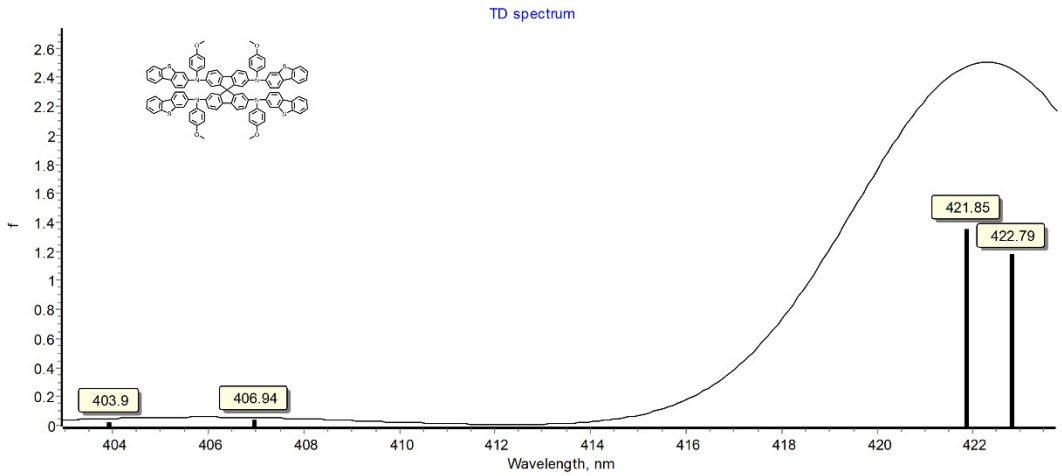

Fig. S1 Calculated absorption spectra of investigated HTMs at the TDDFT/B3LYP/6-311G* level of theory.

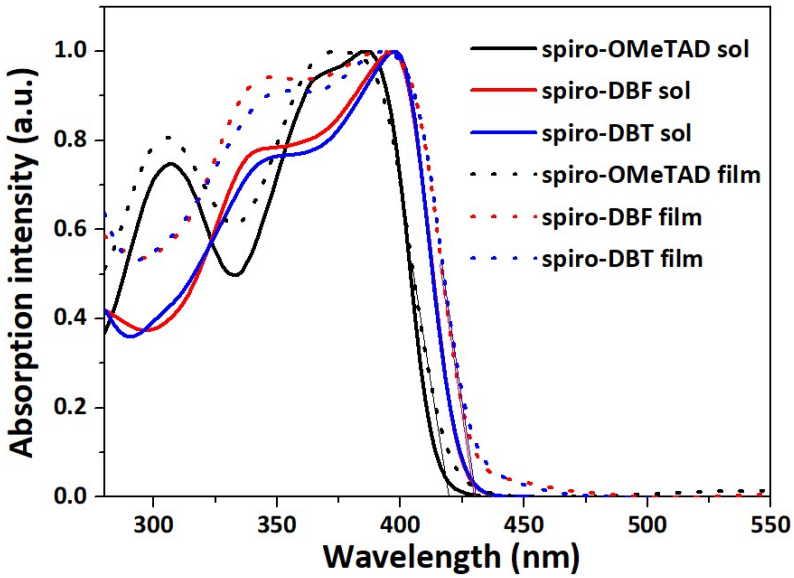

Fig. S2 UV-Vis absorption spectra of spiro-OMeTAD, spiro-DBF, and spiro-DBT in diluted dichloromethane solution and film state.

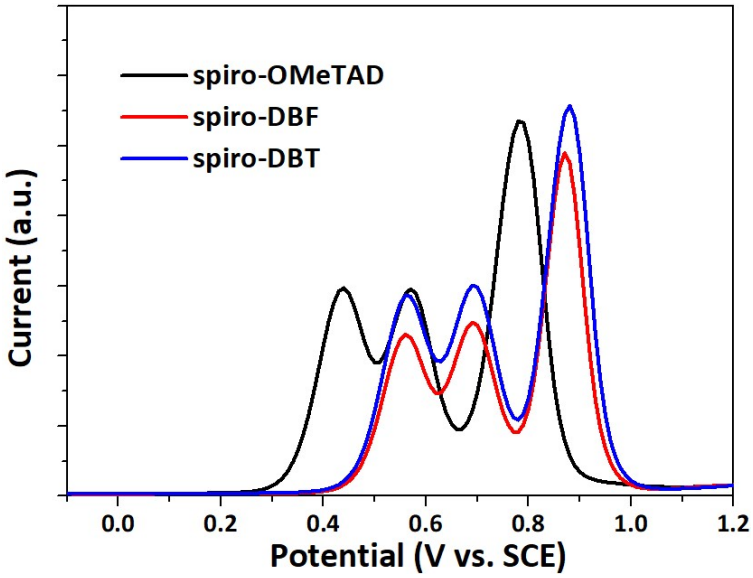

Fig. S3 Differential pulse voltammetry of spiro-OMeTAD, spiro-DBF, and spiro-DBT.

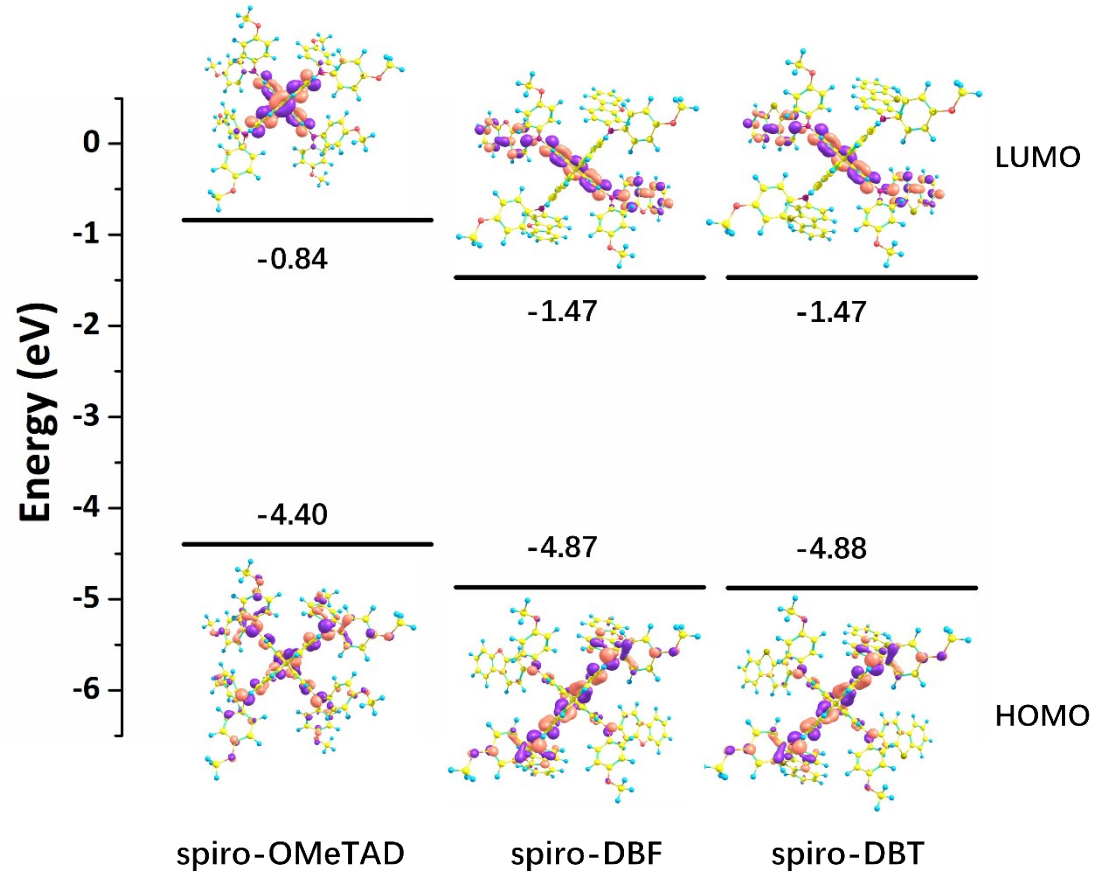

Fig. S4 Calculated electronic structures of HOMO and LUMO levels with spiro-OMeTAD, spiro-DBF and spiro-DBT.

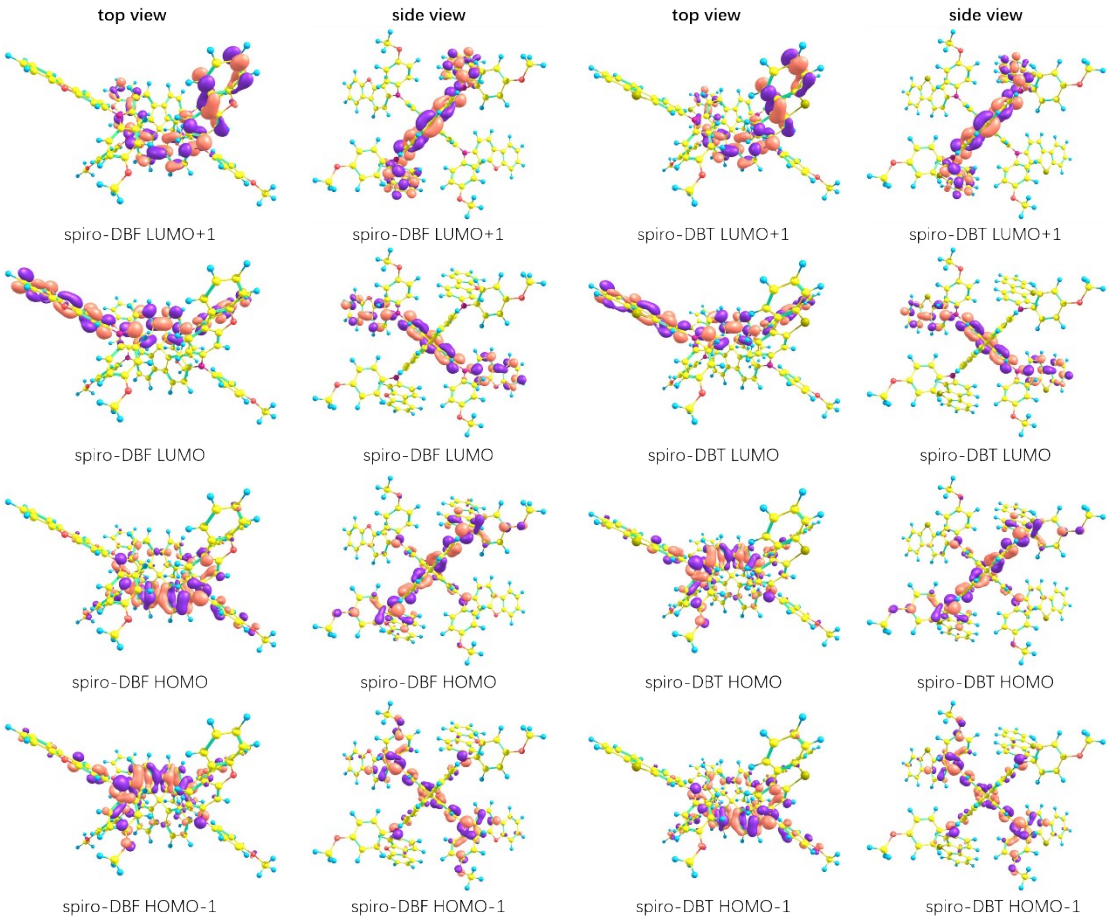

Fig. S5 The detailed molecular orbital distribution of spiro-DBF and spiro-DBT.

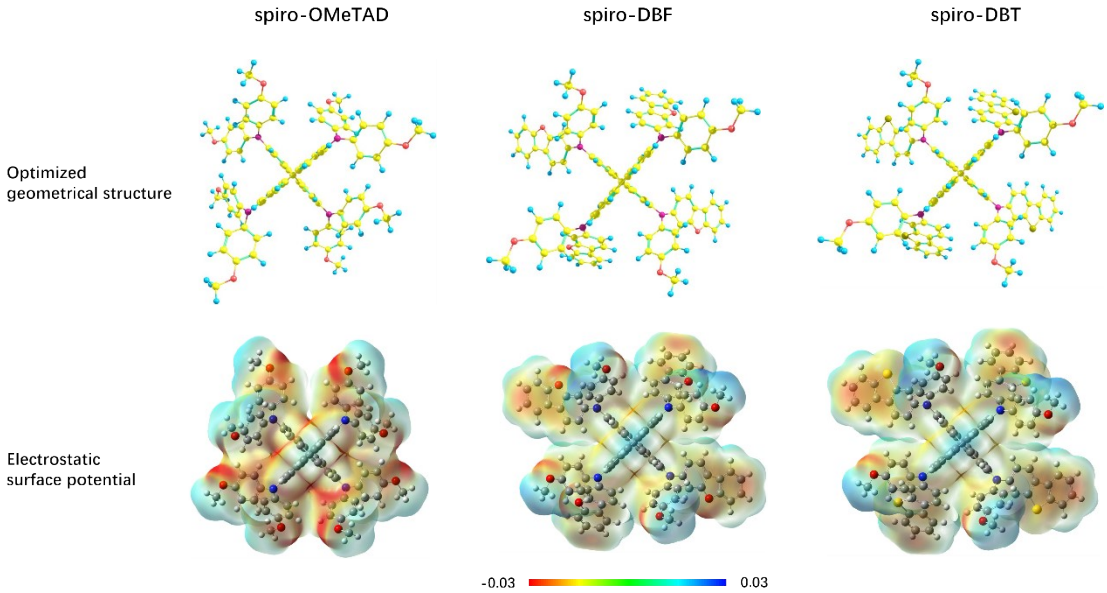

Fig. S6 TDDFT optimized geometry and calculated electrostatic surface potential of spiro-OMeTAD, spiro-DBF and spiro-DBT.

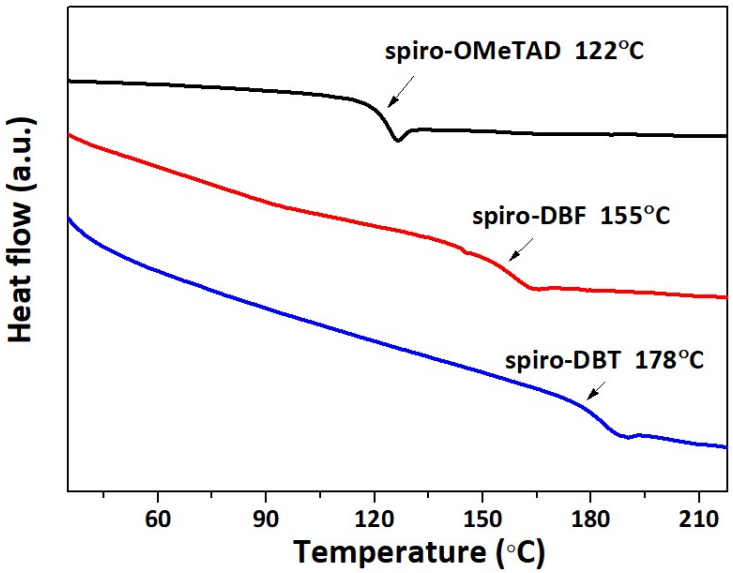

Fig. S7 DSC curves of spiro-OMeTAD, spiro-DBF, and spiro-DBT.

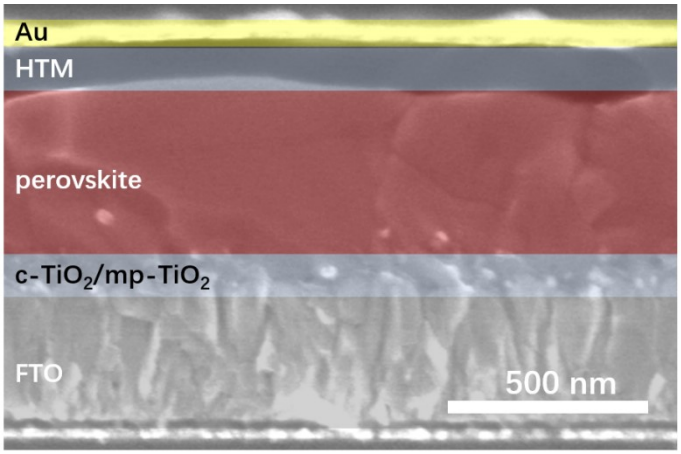

Fig. S8 Cross-sectional SEM image of a PSC.

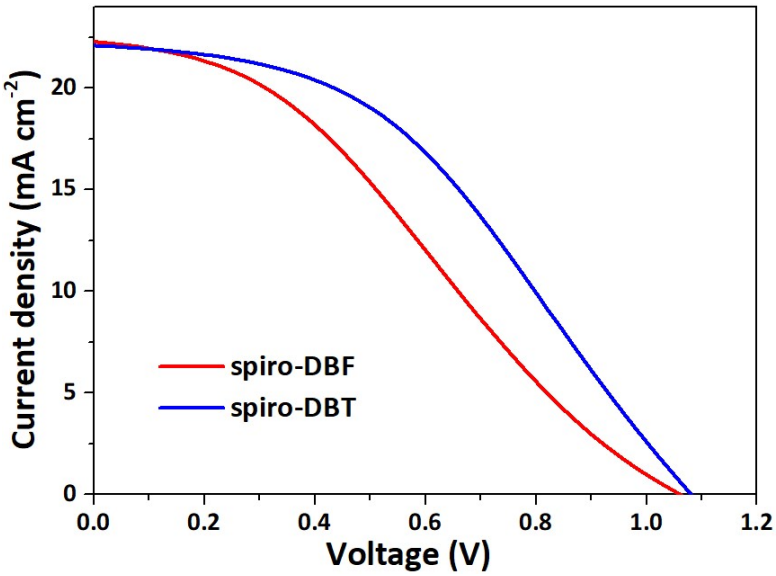

Fig. S9 *J-V* curves of the devices with dopant-free spiro-DBF or spiro-DBT.

Table S1 Photovoltaic parameters of best PSCs employing various HTMs without dopants.

HTM	V_{oc} (V)	J_{sc} (mA cm^{-2})	FF (%)	PCE (%)
spiro-DBF	1.06	22.27	32	7.68
spiro-DBT	1.08	22.09	42	10.09

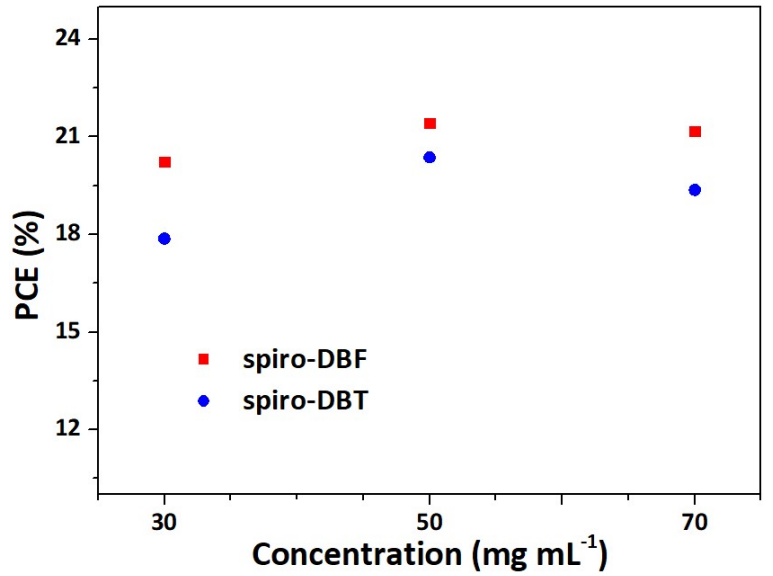

Fig. S10 The PCE variations of the PSCs along with the concentration change of developed HTM (doped).

Table S2 Mean values with standard deviation (STDEV) of photovoltaic parameters (reverse scan direction) of PSCs with different HTMs.

HTM	Concentration (mg mL^{-1})	V_{oc} (V)	J_{sc} (mA cm^{-2})	FF (%)	PCE (%)
spiro-DBF	70	1.10±0.02	24.16±0.20	77±1.2	20.31±0.67
	50	1.12±0.02	24.03±0.19	78±0.9	20.90±0.42
	30	1.07±0.02	23.90±0.20	76±1.1	19.32±0.59
spiro-DBT	70	1.08±0.01	23.90±0.13	73±0.3	18.80±0.22
	50	1.11±0.01	23.58±0.48	76±0.9	19.78±0.54
	30	1.03±0.02	23.55±0.19	69±2.3	16.58±0.98
spiro-OMeTAD	72.3	1.10±0.01	24.08±0.13	77±0.3	20.37±0.22

Notes: The devices with different HTMs contain 8 independent samples.

Table S3 Mean values with standard deviation (STDEV) of photovoltaic parameters (reverse scan direction) of another batch of PSCs (independent batches from table 2) with spiro-DBF (50 mg mL^{-1}) or spiro-OMeTAD.

HTM	V_{oc} (V)	J_{sc} (mA cm^{-2})	FF (%)	PCE (%)
spiro-DBF	1.11±0.02	24.03±0.21	77±1.38	20.66±0.44
spiro-OMeTAD	1.09±0.02	24.09±0.12	76±0.82	19.87±0.38

Notes: The devices with different HTMs contain 16 independent samples.

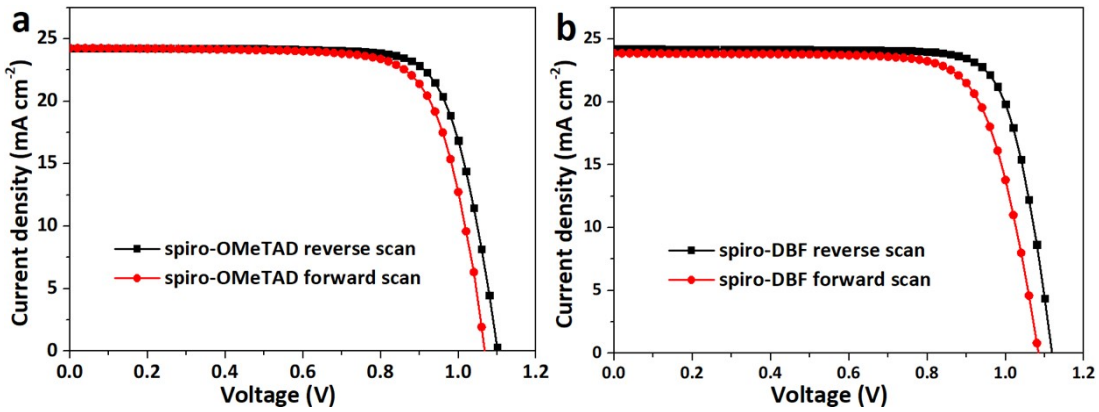

Fig. S11 J-V curves of the devices with spiro-OMeTAD or spiro-DBF as HTMs measured from reverse and forward scans.

Table S4 Photovoltaic parameters of best PSCs with various HTMs and obtained through reverse and forward scans.

HTM	Scan direction	V_{oc} (V)	J_{sc} (mA cm^{-2})	FF (%)	PCE (%)	HI (%)
spiro-OMeTAD	Reverse	1.10	24.25	77	20.56	5.5
	Forward	1.07	24.26	75	19.42	
spiro-DBF	Reverse	1.12	24.21	79	21.43	9.2
	Forward	1.08	24.18	75	19.45	

HI = ($PCE_{reverse}$ - $PCE_{forward}$)/$PCE_{reverse}$

Table S5 TRPL parameters of perovskite films with different HTMs.

HTM	A1 (%)	*τ1 (ns)*	A2 (%)	*τ2 (ns)*	average *τ*
Perovskite (P)	11.5	1	88.5	20	18
P/spiro-OMeTAD	28.3	1	71.7	14	10
P/spiro-DBF	38.1	1	61.9	11	7
P/spiro-DBT	22.2	1	77.8	18	14

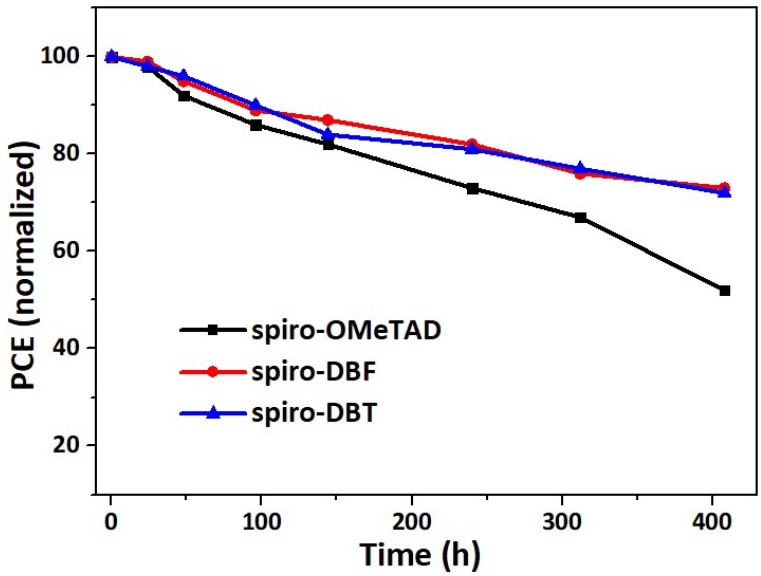

Fig. S12 The stability of the devices based on different HTMs without encapsulation (around 60% relative humidity).

Experimental Section

Device Fabrication

Firstly, FTO glass plates were sequentially cleaned by stain remover, deionized water and ethanol with ultrasonic bath. By using spray pyrolysis methods, the compact TiO_2 layer was deposited on the clean FTO substrate at 500 °C in which a precursor solution of 0.6 mL titanium diisopropoxide dissolved in 14 mL Ethanol. Mesoporous TiO_2 layer was deposited on above obtained substrate by spin-coating of a diluted particle TiO_2 paste (Dyesol 30NR-T, 1:12 w/w diluted in ethanol) at 3000 rpm for 30 s. Subsequently, the substrates were annealed at around 500 °C for 40 min. After cooling down, the perovskite layer was deposited through spin-coating the perovskite precursor solution by a one-step solvent engineering procedure. Perovskite precursor solutions (1.4M) with a composition of $(CsPbI_3)_{0.05}(FAPbI_3)_{0.95}$ and 30 mol% MACl in DMF/DMSO mixed solvent (1000 µL, volume ratio 4:1).[1] The spin-coating procedure was performed first 1000 rpm for 10 sand second 5000 rpm for 30 s. Then 110 µL chlorobenzene was dripped on the spinning substrate during the second spin-coating step 10 s at the end of the procedure. The obtained substrate was immediately heated at 100 °C for 0.5 h

and 150 °C for 10min on the hotplate. The HTM was subsequently deposited on the FTO/bl-TiO_2/mp-TiO_2/perovskite substrate by spin-coating at 5000 rpm for 30 s after above substrate cooling to R.T.. The HTM solution was prepared in anhydrous chlorobenzene, the concentration is 50 mg mL^{-1} for dopant-free HTMs. For doped HTMs, the concentration is 70, 50 and 30 mg mL^{-1}, respectively. For 70 mg mL^{-1} of HTMs, which is doped with 15 μL of 4-tert-butylpyridine and 9 μL of lithium bis(trifluoromethylsulphonyl)imide (520 mg mL^{-1} in acetonitrile) and 4 μL tris (2-(1H-pyrazol-1-yl)-4-tert-butyl-pyridine)-cobalt(III) tris (bis (trifluoromethylsulfonyl) imide) (300 mg mL^{-1} in acetonitrile). The HTMs with low concentration were obtained by gradual diluting the HTMs with high concentration. Spiro-OMeTAD (99.8%, HPLC, Xi'an Polymer Light Technology Corp.) were dissolved in chlorobenzene (72.3 mg mL^{-1}) with 15 μL of 4-tert-butylpyridine and 9 μL of lithium bis(trifluoromethylsulphonyl)imide (520 mg mL^{-1} in acetonitrile) and 4 μL tris (2-(1H-pyrazol-1-yl)-4-tert-butyl-pyridine)-cobalt(III) tris (bis (trifluoromethylsulfonyl) imide) (300 mg mL^{-1} in acetonitrile). Finally, a ~70 nm thick Au counter electrode was deposited on top of above film by thermal evaporation. The active area of the device was defined by a black mask with a size of 0.1225 cm^2 for all measurements.

Characterization

NMR spectra were recorded on a Brücker spectrometer (400 or 500 MHz) with chemical shifts against tetramethylsilane (TMS). UV-vis spectra of investigated molecules are carried out on a UV-vis spectrophotometer (UV-3600 plus, Shimadzu Co. Ltd, Japan). The PL measurements of HTM were recorded on the fluorescence spectrophotometer (Hitachi F-4600, Japan). Differential scanning calorimetry is carried out with a scan rate of 15 $^oC\ min^{-1}$ (METTLER-Toledo DSC1). The PL spectrum of perovskite/HTM films were obtained from a fluorescence spectrometer (FLS980, Edinburgh, UK) with the excitation wavelength of 488 nm. Cyclic voltammetry was tested with a CHI660d electrochemical analyzer (CH Instruments, Inc., China). A normal three electrode system was used consisting of a platinum wire counter electrode, a platinum working electrode, as well as a calomel reference electrode. Redox potential of investigated compounds was tested in DCM with 0.1 M tetrabutylammonium hexafluorophosphate with a scan rate of 50 mV s^{-1}. The film morphology was measured by atomic force microscopy (5500AFM, Agilent Technologies, USA). The *J–V* characteristics were carried out using a Keithley 2400 source meter under AM 1.5G and a 3A grade solar simulator (Newport, USA) with an intensity of 100 mW cm^{-2}. The incident photon-to-current conversion efficiency (IPCE) was recorded on QE/IPCE measurement kit (Sofn Instruments Co., LTD, China). The moisture resistance of HTMs was measured on a contact angle tester (METATEST E3-300).

The charge carrier mobility of the HTM films was measured using the space-charge-limited current (SCLC) technique. Hole-only devices were fabricated in a structure of ITO/PEDOT:PSS/HTM/Au. The device characteristics were extracted by modeling the dark current under forward bias using the SCLC expression described by the Mott-Gurney law:

$$J = \frac{9}{8}\varepsilon_r \varepsilon_0 \mu \frac{V^2}{L^3}$$

Here, $\varepsilon_r = 3$ is the average dielectric constant of the film, ε_0 is the permittivity of the free space, μ is the carrier mobility, L is the thickness of the film, and V is the applied voltage.

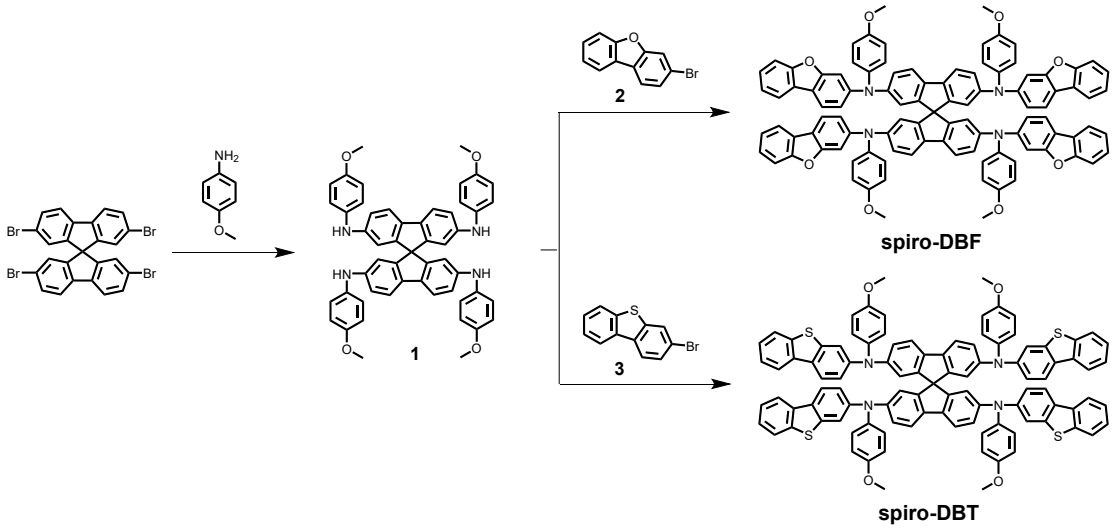

Scheme S1 Synthesis procedures of spiro-DBF and spiro-DBT.

Synthesis

Compound 1 was mainly synthesized according to previous report with an optimized process in our lab.[2 3]

spiro-DBF

Compound 1 (0.3 mmol, 240 mg), compound 2 (3-bromodibenzofuran, 1.8 mmol, 480 mg), potassium tert-butoxide (0.9 g, 8 mmol), $Pd(OAc)_2$ (112 mg, 0.5 mmol), $P(tBu)_3$ (0.1 M in toluene, 0.5 mL) were added into a 50 mL flask and degassed using Ar. Then 30 mL dry toluene was injected in to the flask and degassed using Ar. The reaction solution was kept with stirring at reflux for 48 h. After cooling to R.T., the mixture was diluted by 30 mL CH_2Cl_2 and washed with 50 mL deionized water for 3 times. The organic phase was dried by Na_2SO_4, and removed solvent using a rotary evaporator. After drying, the solid is purified by column chromatography (CH_2Cl_2/PE = 3:1) to obtain the product as canary yellow solid which was washed several times with the mixed solvent of ethyl acetate and petroleum ether. ^{1}H NMR (400 MHz, DMSO-d_6) δ 7.96 (d, *J* = 7.4 Hz, 4H), 7.86 (d, *J* = 8.4 Hz, 4H), 7.56 (d, *J* = 8.2 Hz, 4H), 7.50 (d, *J* = 8.1 Hz, 4H), 7.37 (t, *J* = 7.5 Hz, 4H), 7.31 (t, *J* = 7.5 Hz, 4H), 7.16 – 6.94 (m, 14H), 6.87 (m, 14H), 6.46 (s, 4H), 3.73 (s, 12H). ^{13}C NMR (125 MHz, DMSO-d_6) δ 156.92, 156.65, 156.10, 149.87, 148.14, 146.99, 139.99, 135.84, 127.58, 126.64, 124.11, 123.69,

123.42, 121.60, 121.27, 120.58, 118.25, 117.94, 117.72, 115.39, 111.60, 104.39, 65.50, 55.55. Anal. Calcd. for C101H68N4O8 (%): C, 82.77; H, 4.68; N, 3.82. Found: C, 82.75; H, 4.69; N, 3.80. HRMS (ESI) *m/z*: [M+] calcd, 1465.5071; found 1465.5083.

spiro-DBT

spiro-DBT was synthesized following the same procedure to prepare spiro-DBF. Compound 3 (3-bromo-dibenzothiophene, 1.8 mmol, 470 mg) was used instead of compound 2. ^{1}H NMR (400 MHz, DMSO-d_6) δ 8.15 (d, *J* = 7.2 Hz, 4H), 8.07 (d, *J* = 8.6 Hz, 4H), 7.90 (d, *J* = 7.4 Hz, 4H), 7.52 (d, *J* = 8.2 Hz, 4H), 7.48 – 7.31 (m, 12H), 7.11 – 6.94 (m, 12H), 6.88 (m, 12H), 6.45 (s, 4H), 3.73 (s, 12H). ^{13}C NMR (125 MHz, DMSO-d_6) δ 156.67, 149.81, 147.31, 146.94, 140.37, 139.93, 138.47, 135.65, 135.32, 129.68, 127.70, 126.38, 125.10, 123.29, 123.23, 122.74, 121.57, 121.21, 119.90, 117.80, 115.43, 115.17, 65.55, 55.58. Anal. Calcd. for $C_{101}H_{68}N_4O_4S_4$ (%): C, 79.29; H, 4.48; N, 3.66; S, 8.38. Found: C, 79.27; H, 4.49; N, 3.65; S, 8.36. HRMS (ESI) *m/z*: [M+] calcd, 1529.4157; found 1529.4179.

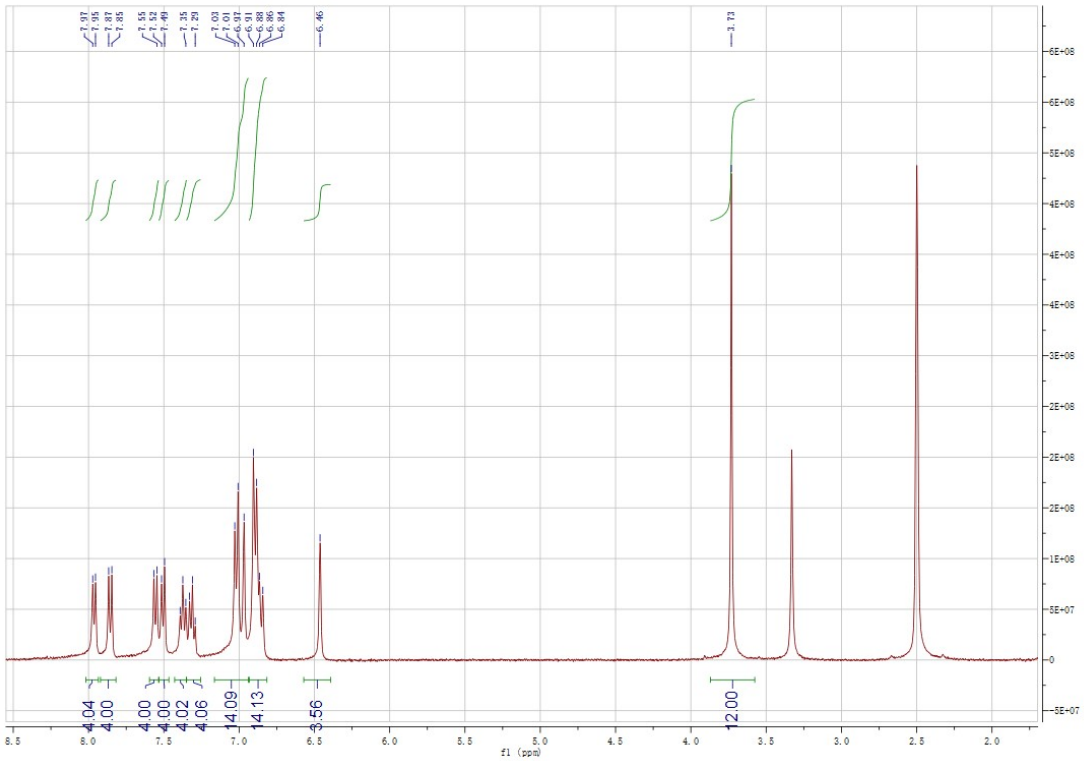

Fig. S13 1H NMR of spiro-DBF.

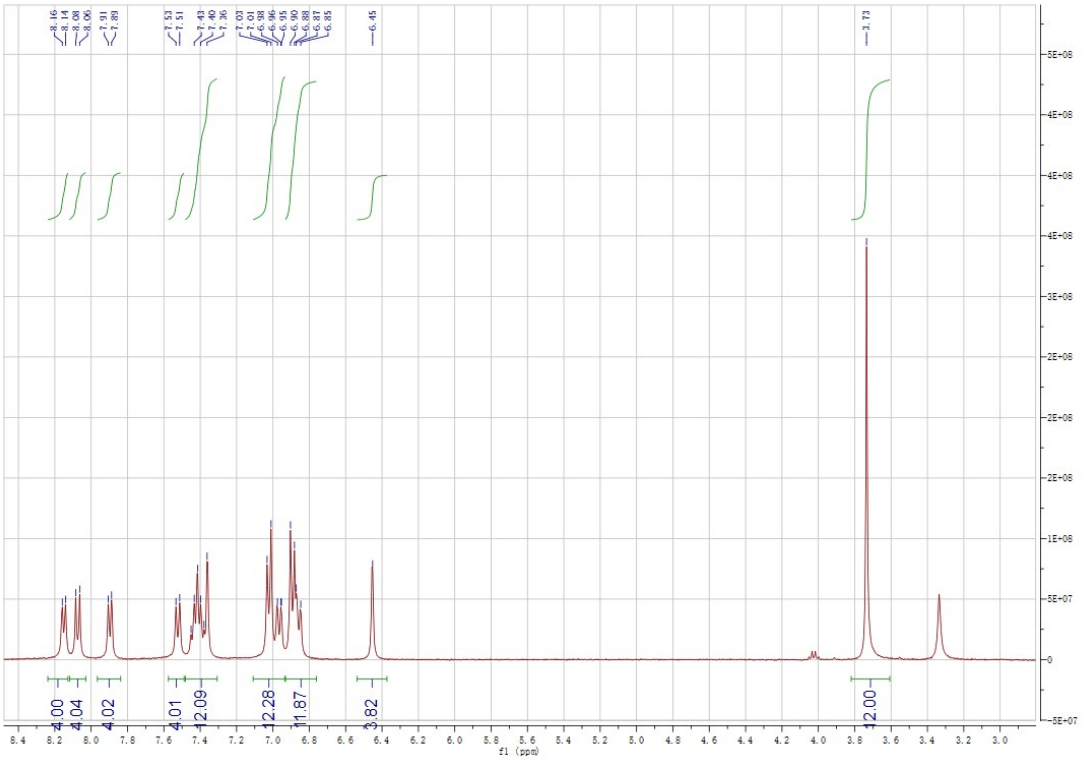

Fig. S14 1H NMR of spiro-DBT.

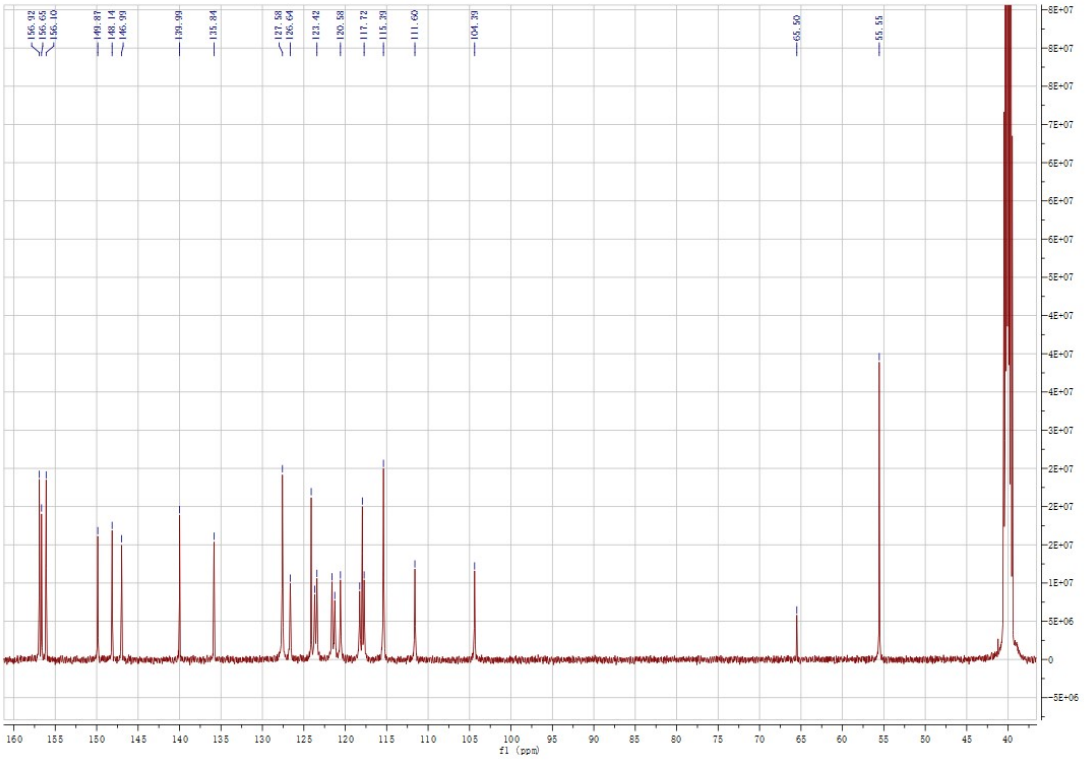

Fig. S15 ^{13}C NMR of spiro-DBF.

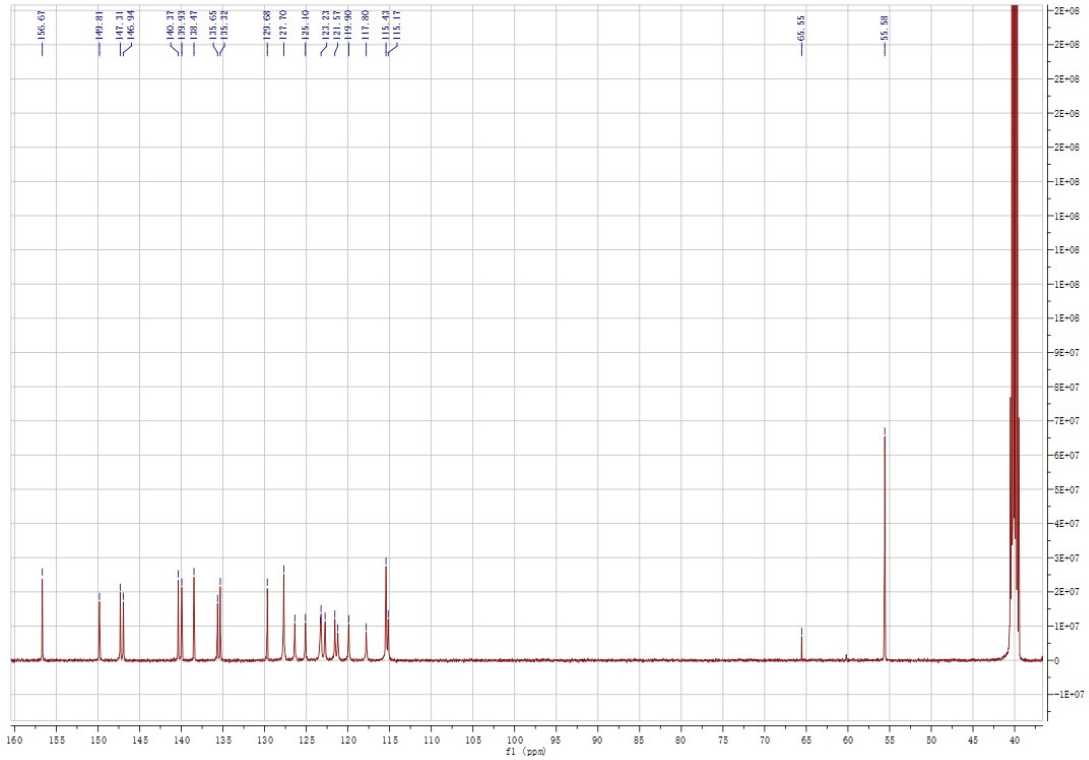

Fig. S16 ^{13}C NMR of spiro-DBT.

References

1. T. Niu, W. Zhu, Y. Zhang, Q. Xue, X. Jiao, Z. Wang, Y.-M. Xie, P. Li, R. Chen, F. Huang, Y. Li, H. L. Yip and Y. Cao, *Joule*, 2021, **5**, 249-269.
2. X. Zhang, X. Liu, N. Wu, R. Ghadari, M. Han, Y. Wang, Y. Ding, M. Cai, Z. Qu and S. Dai, *J. Energy Chem.*, 2022, **67**, 19-26.
3. N. J. Jeon, H. Na, E. H. Jung, T.-Y. Yang, Y. G. Lee, G. Kim, H.-W. Shin, S. I. Seok, J. Lee and J. Seo, *Nat. Energy*, 2018, **3**, 682-689.